

# TTF-FEL Photoinjector Simulation giving a High Quality Beam

J. L. Coacolo, C. Pagani, L. Serafini  
 INFN Milano  
 Lab. L.A.S.A.  
 Via F. Cervi 201  
 20090 Segrate (Milano), Italy

February 23, 1996

## Abstract

In this paper we present a study of the beam quality at the TESLA FEL photoinjector exit. The beam dynamics is simulated by ATRAP which is a 2D1/2 numerical code using the Lienard-Wiechert potential to calculate the space charge force. For this study the injector geometry and the magnetic field are given by Klaus Floettmann. We don't take into account the thermal emittance in the beam dynamics, because we don't know the energy and velocity profile at the cathode exit. But, with some assumptions, we find that it can be the major part of the transverse emittance.

## 1 Introduction

The TESLA FEL needs to develop a photoinjector giving a high quality beam. We need at the gun exit a radial rms emittance  $\epsilon_r < 1 \text{ mm.mrad}$ , and a longitudinal rms emittance  $\epsilon_z < 20 \text{ mm.KeV}$ . To obtain these, Klaus Floetmann propose a gun, figure 1, with a coaxial input coupler. The rf field and the magnetic field distributions on the axis are shown in the figures 2 and 3.

The quality optimisation is all the more difficult since many parameters play a role in the beam dynamics. Fortunately we have some constraints given by the project : the beam charge is 1 nC, the micro pulse rise time of the laser Nd:YLF is 5 ps then the pulse length  $\sigma_t = 3 \text{ ps}$ . Furthermore, the rf peak field on the cathode must be high enough to limit the space charge effects on the beam quality, but not too high to avoid a too strong defocusing effect of the rf field. For this, we have taken the peak field  $E_0 = 50 \text{ MV/m}$ .

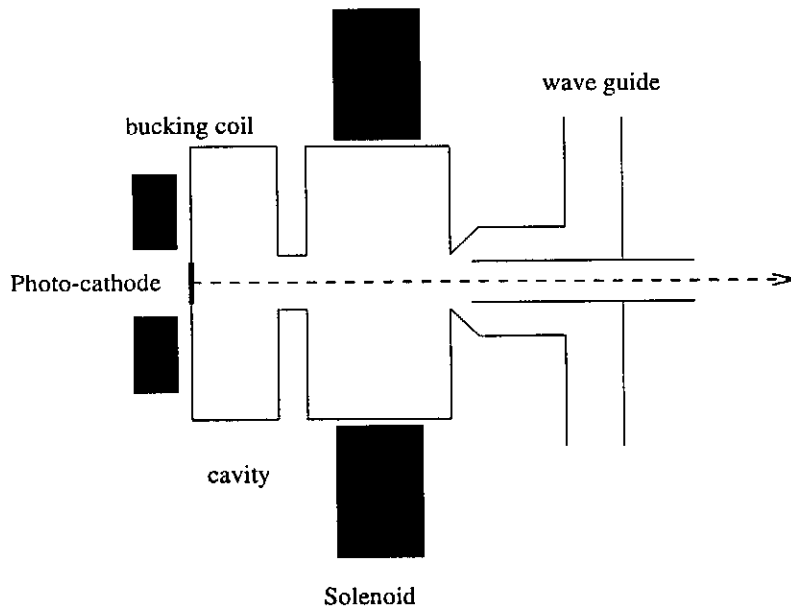


Figure 1: General scheme of the TESLA FEL gun.

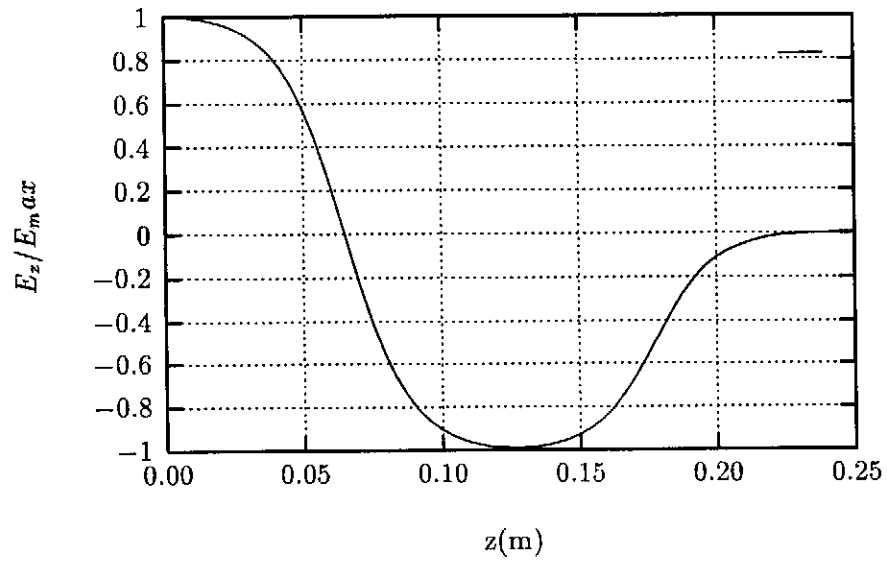


Figure 2: On axis normalised rf field in the 1.5 cell.

The parameter set optimising the beam quality, given in this paper, is adapted to this gun. For example, with this type of cavity, i.e the first half cell greater than  $\frac{\lambda}{4}$  with  $\lambda$  the wave length of the rf field, the rf phase is close to  $-35^\circ$  when the beam center leaves the cathode. Then the rf field seen by the electrons at the cathode exit, for a 50 MV/m peak field is close to 40 MV/m. If the first half cell is  $\frac{\lambda}{4}$ , this field becomes 45 MV/m, and the space charge effect decreases. Furthermore, we can expect to have a best power stability if we take a cavity with two cells and half. So for a refined study, we will have to see the influence of the rf field and magnetic field distribution, the number of cells, etc... This will be the subject of the next report.

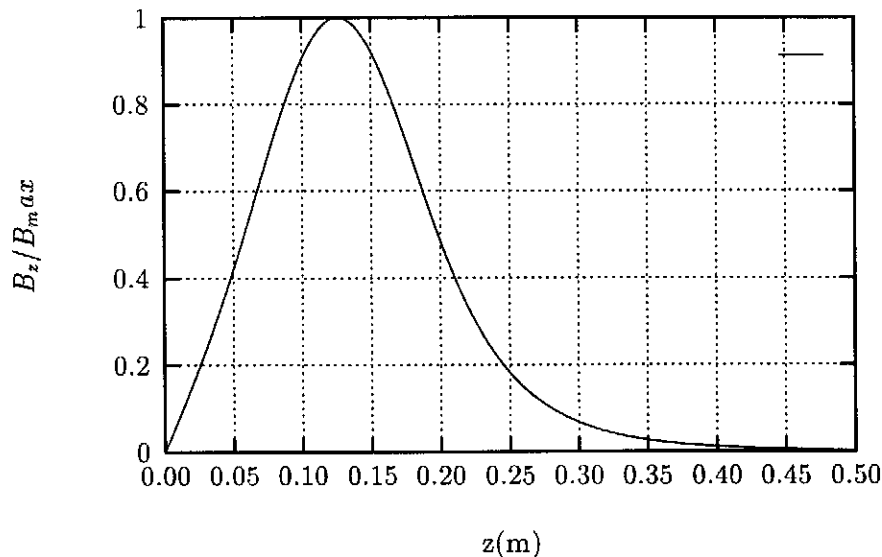


Figure 3: Normalised magnetic field on the axis due to the solenoid and the bucking coil.

To optimise the transverse emittance, we know that a uniform distribution for the electron beam is better than a gaussian distribution. Unfortunately the temporal distribution of the laser beam is close to a gaussian. If we take a longitudinal superposition of pulses, we can have a near flat top distribution. We have chosen a superposition of 3 pulses, because it is the minimum number to have a respectable flat top distribution, and it is a reasonable number of pulses to obtain a length of 50  $\mu\text{m}$  after the magnetic compression.

We define a uniform charge density in radius, which is achievable in reality. In fact the radial profile is a truncated gaussian, and to have a uniform profile, a part of the laser energy is lost. For this, it would be interesting to see the influence of a truncated gaussian distribution on the beam quality. We have taken three cases for the longitudinal distribution: the first is a uniform distribution, the second is a short flat top distribution (figure 4) and in the third, we take into account some fluctuations,  $\pm 5\%$  on the flat top (figure 5), which is the more realistic case. The different parameters are summarized in the table 1.

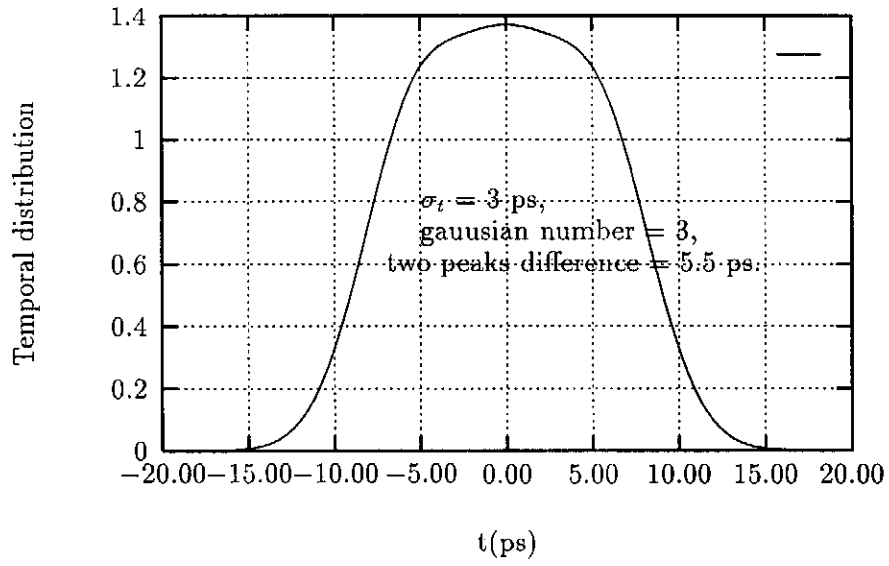


Figure 4: Beam temporal distribution, case 2.

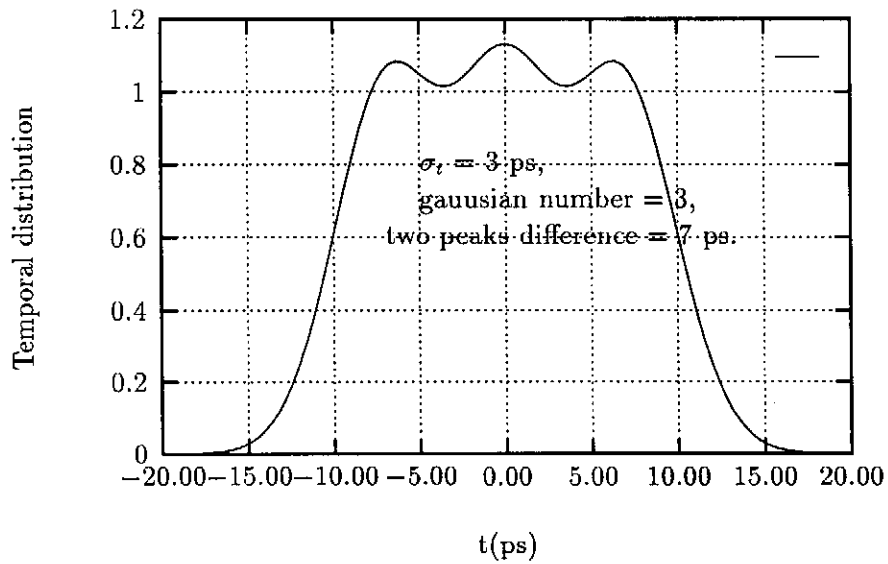


Figure 5: Beam temporal distribution, case 3.

Table 1: The ATRAP simulation parameters.

Charge	1 nC
$E_0$	50 MV/m
Initial thermal emittance	0. mm.mrad
Radial profile	uniform
Temporal profile	
case 1	uniform
	Launch phase <sup>(1)</sup> -31°
	$\tau$ 12 ps
case 2	gaussians superposition
	Launch phase <sup>(1)</sup> -34°
	number 3
	$\sigma_t$ 3 ps
	$\Delta peak^{(2)}$ 5.5 ps
case 3	gaussians superposition
	Launch phase <sup>(1)</sup> -34°
	number 3
	$\sigma_t$ 3 ps
	$\Delta peak^{(2)}$ 7 ps

(1) Launch phase is the phase gap between the beam center exit and the maximum peak field on the cathode.

(2)  $\Delta peak$  is the gap between two gaussians centers.

## 2 Transverse rms emittance

In the wiggler, we can consider that the particles of the beam tails don't contribute to the radiation, because the current isn't high enough. For this, it is attractive to calculate the transverse emittance by three methods. The first, take into account all the electrons, the second and the third, 80% and 50% of the length. For the gaussians superposition the length is defined by  $2*(\Delta peak + 3\sigma_t)$ .

To have  $\epsilon_r = \epsilon_x$ , the definition of the transverse rms emittance is :

$$\epsilon_r = \frac{1}{2mc} \sqrt{\langle r^2 \rangle \langle pr^2 \rangle - \langle rpr \rangle^2} \quad (1)$$

## 2.1 Total length

### - Uniform temporal profile.

In figure 6, the minimum value of  $\epsilon_r$  in the drift space, is plotted for different beam radii and solenoid field. We can see that  $\epsilon_r$  is very sensitive to the magnetic field. This sensitivity increase with the radius. Furthermore we can see that for  $R = 2.5$  mm there is an absolute minimum which is 0.65 mm.mrad. There are two competitive mechanisms, the first is the rf emittance which increases with the radius, and the second is the space charge emittance which decreases with the radius.

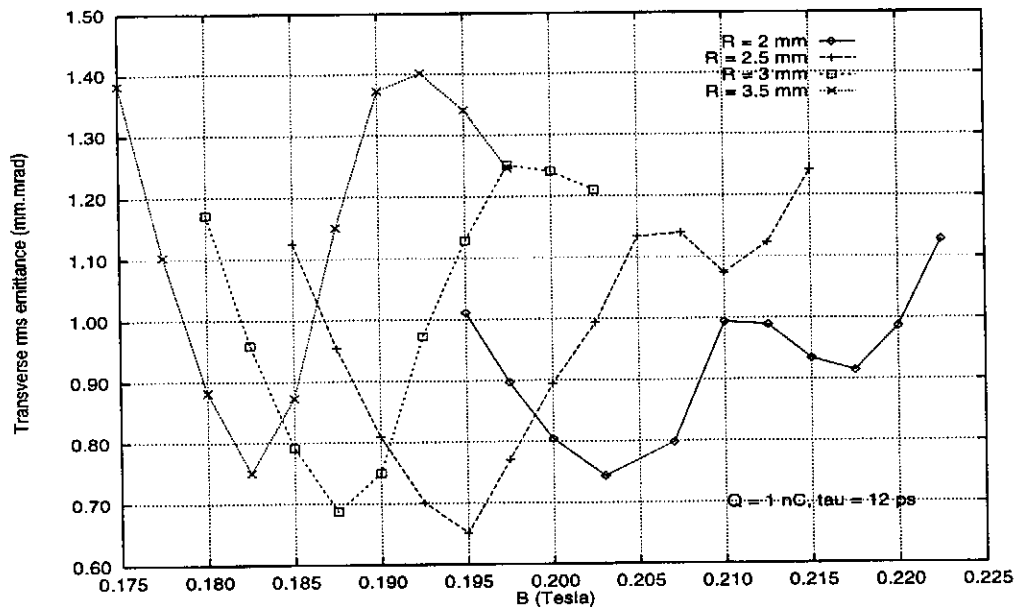


Figure 6: Minimum Transverse rms emittance versus the magnetic peak field.

### - Gaussian superposition, $\Delta_{peak} = 5.5$ ps.

For the figure 7, the same remarks can be done. Nevertheless, we can note a greater sensitivity to the magnetic field, than the last case, and a second local minimum which appears when the magnetic field increases. This minimum corresponds to an over focusing magnetic field, and we can see, in the figure 8 for the case  $R = 2$  mm and  $B = 0.22$  Tesla, an unstable solution. Afterwards, we will consider only the first minimum, for the smallest value of the magnetic field. The emittance minimum is close to 1.7 mm.mrad, for  $1. < R < 1.5$  mm, which is greater than the acceptable limit.

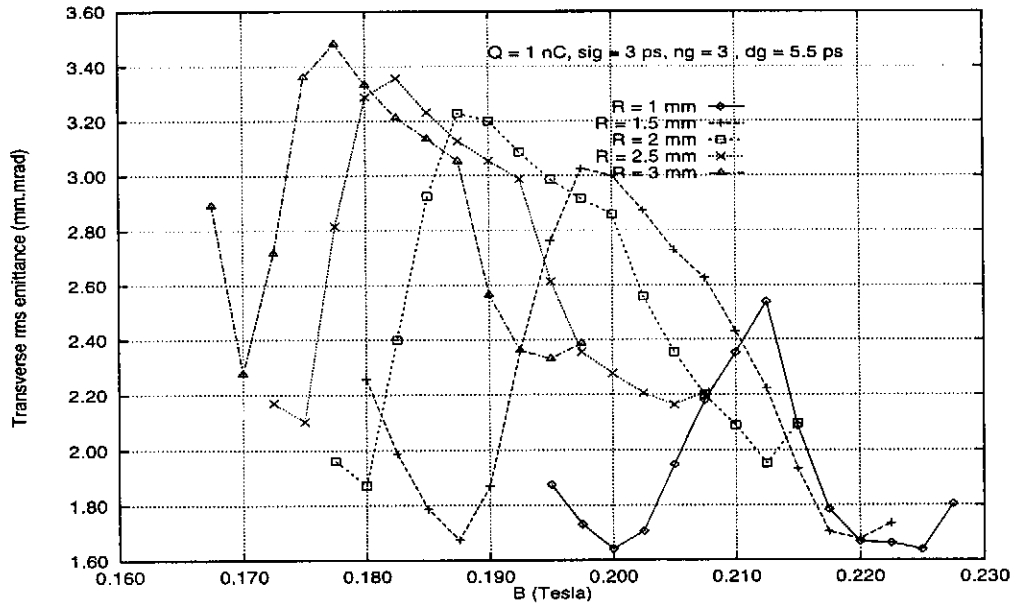


Figure 7: Minimum Transverse rms emittance versus the magnetic peak field.

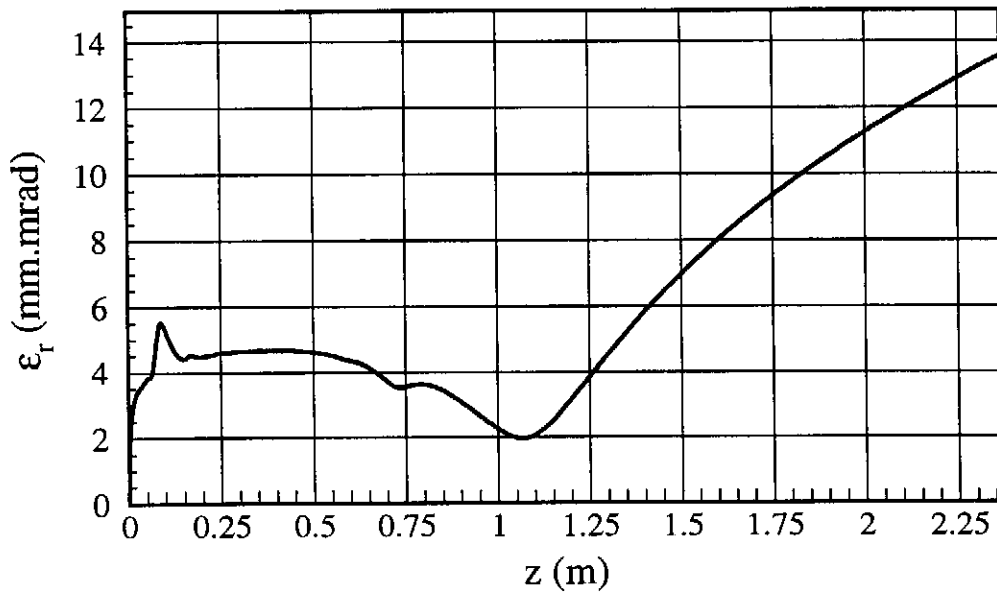


Figure 8: Transverse rms emittance versus the position.

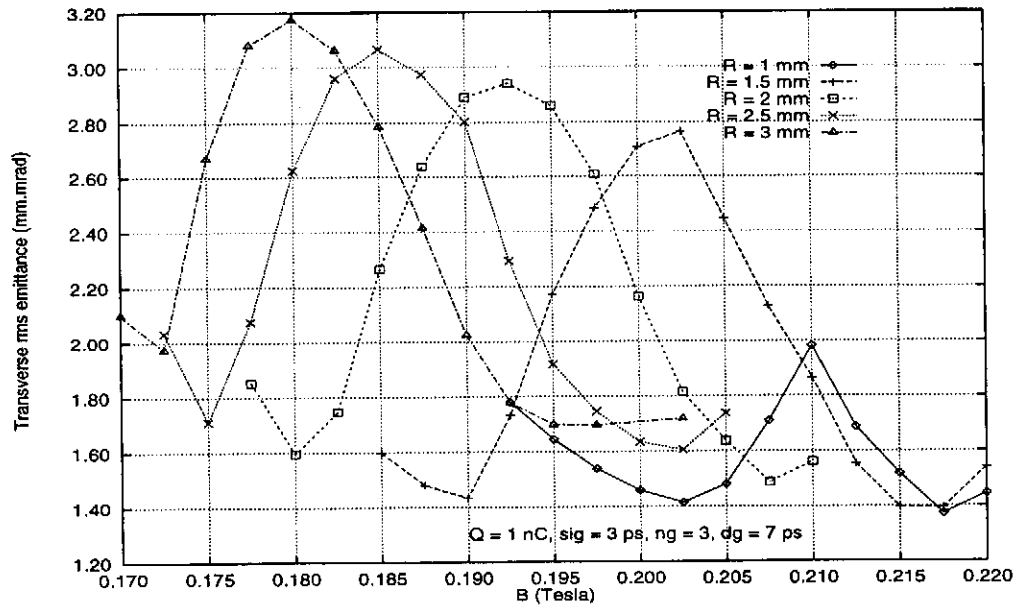


Figure 9: Minimum Transverse rms emittance versus the magnetic peak field.

- Gaussian superposition,  $\Delta_{peak} = 7$  ps.

For this case (see figure 9) the curves evolution is the same as "case 2". The minimum is better, here we have  $\epsilon_r = 1.4$  mm.mrad for  $R = 1.5$  mm and  $B = 0.19$  Tesla. In fact, the temporal profile of "case 2" is close to a gaussian profile, which increases the emittance.

## 2.2 80% of the length

- Case 1.

Figure 10 shows the evolution of minimum  $\epsilon_r$  for 80% of the beam length or approximately 98% of the charge as a function of the magnetic peak field. It seems that the best case is for  $R = 3$  mm, and  $\epsilon_r = 0.35$  mm.mrad, moreover there is not a great difference, between this case and  $R = 2.5$  and  $3.5$  mm.

- Case 2.

We can see in the figure 11, that with 80% of the length or 98% of the charge, we can reach 1.2 mm.mrad for  $\epsilon_r$  instead of 1.7 mm.mrad for the total length. It is interesting to see that only 2% of the charge doesn't contribute and  $\epsilon_r$  becomes 70% of the total emittance.



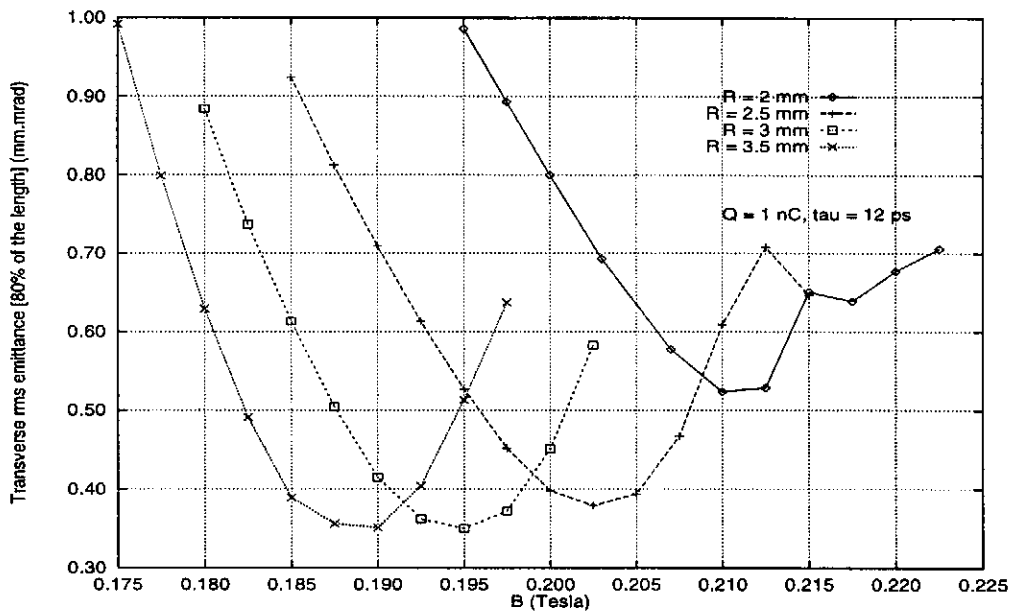


Figure 10: Minimum Transverse rms emittance, 80% of the length, versus the magnetic peak field.

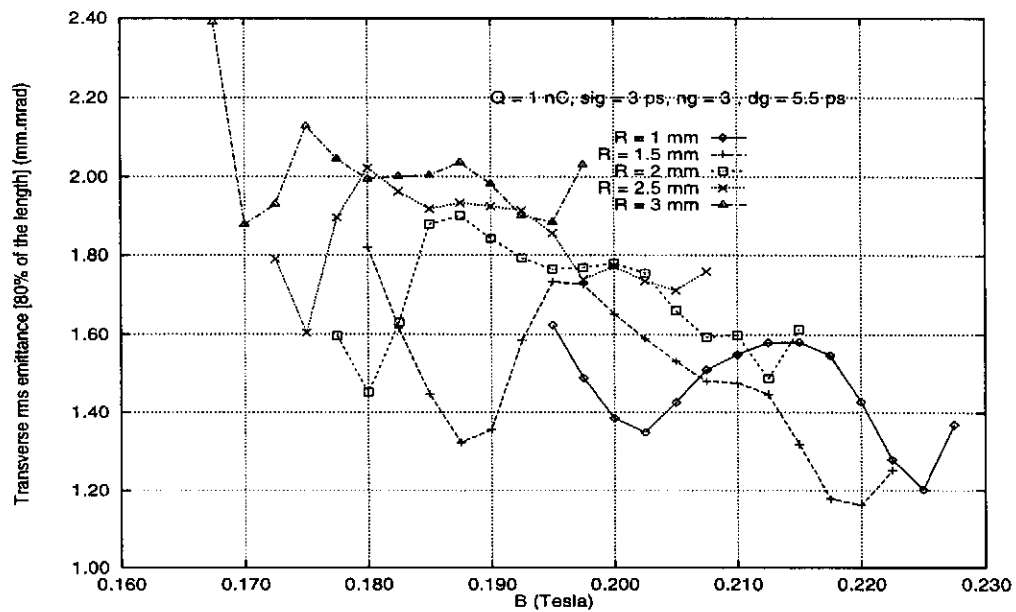


Figure 11: Minimum Transverse rms emittance, 80% of the length, versus the magnetic peak field.

- Case 3.

In figure 12, we reach 1 mm.mrad for  $R = 1.5$  mm and 0.19 Tesla for the magnetic peak field.

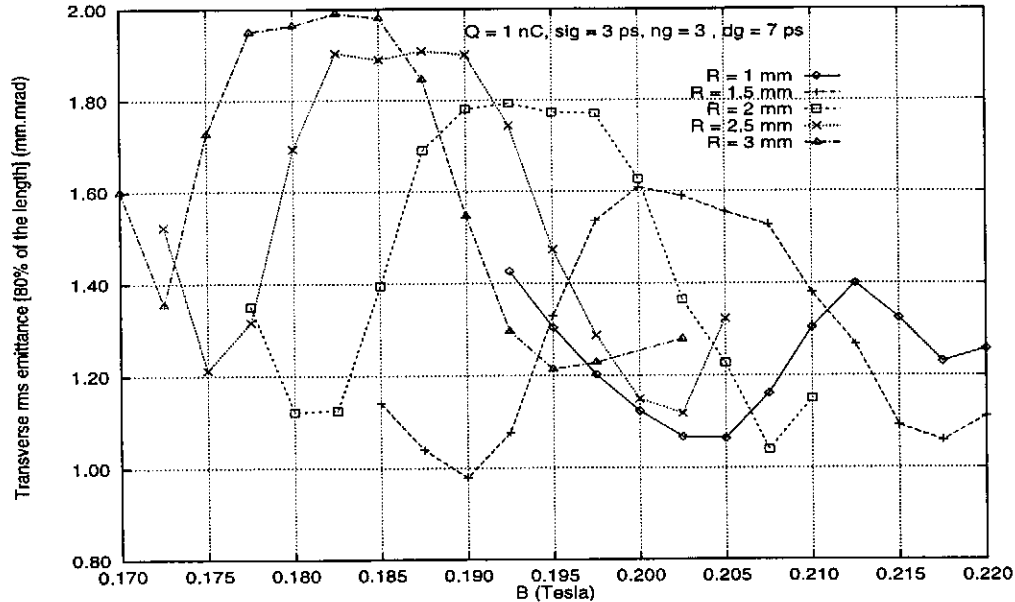


Figure 12: Minimum Transverse rms emittance, 80% of the length, versus the magnetic peak field.

## 2.3 50% of the length

- Cases 1.

In this part we consider the first case, just to see the emittance evolution in function of the truncated part of the beam (it is clear that more than 50% of the beam length contribute to the radiation). Figure 15 shows a minimum close to 0.15 mm.mrad.

- Cases 2,3.

The 50% of the beam length is shown in the figures 13,14 between the two vertical lines which represent respectively 0.8 and 0.75 nC. In figures 16,17 is plotted the minimum transverse rms emittance versus the magnetic peak field. For the case 2, the minimum is between 0.5 and 0.6 mm.mrad, if we consider only the points before the cross over. For the case 3, the minimum is closed to 0.45 mm.mrad and stable with the magnetic field. This is very attractive, because we can optimise the longitudinal emittance without change the transverse emittance. To have 1 nC in 50% beam length, for the case 3, we

have taken 1.3 nC for the charge beam and we obtain  $\epsilon_r = 0.59$  mm.mrad for  $B = 0.1925$  Tesla and  $\epsilon_r = 0.53$  mm.mrad for  $B = 0.1975$  Tesla.

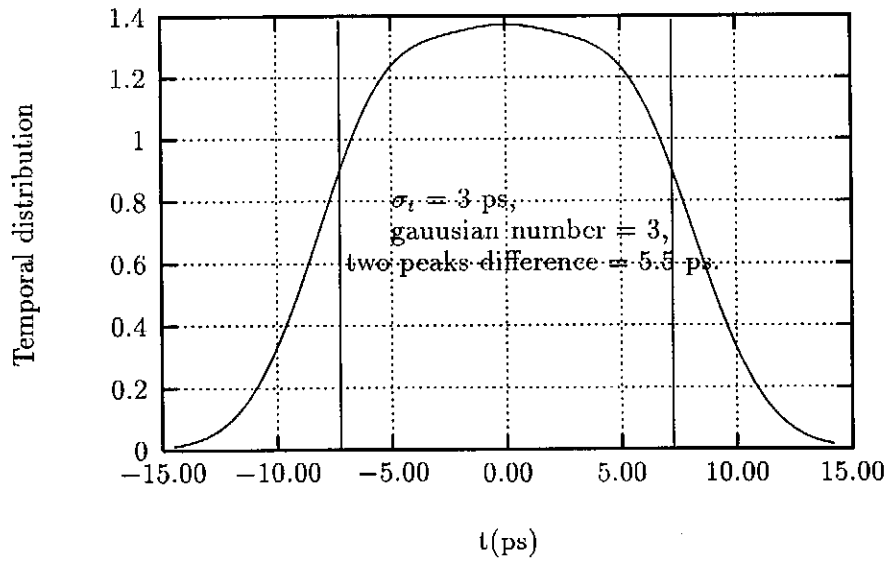


Figure 13: Case 2, 50% of the length is between the two vertical lines.

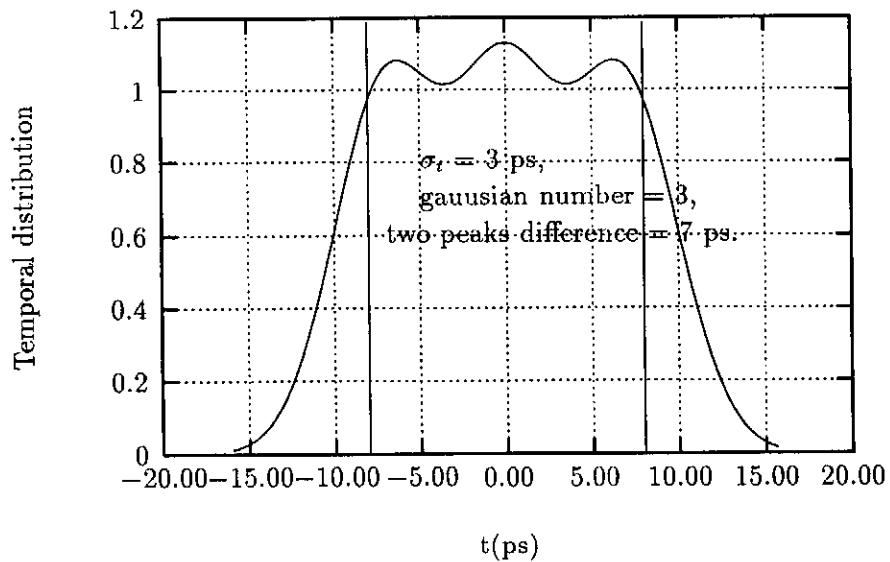


Figure 14: Case 2, 50% of the length is between the two vertical lines.

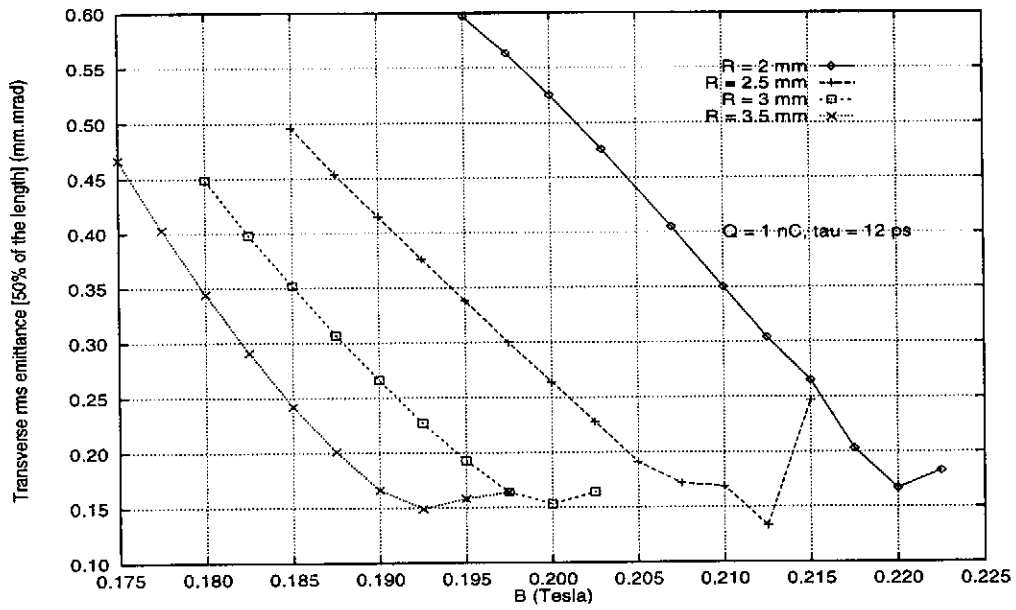


Figure 15: Minimum Transverse rms emittance, 50% of the length, versus the magnetic peak field.

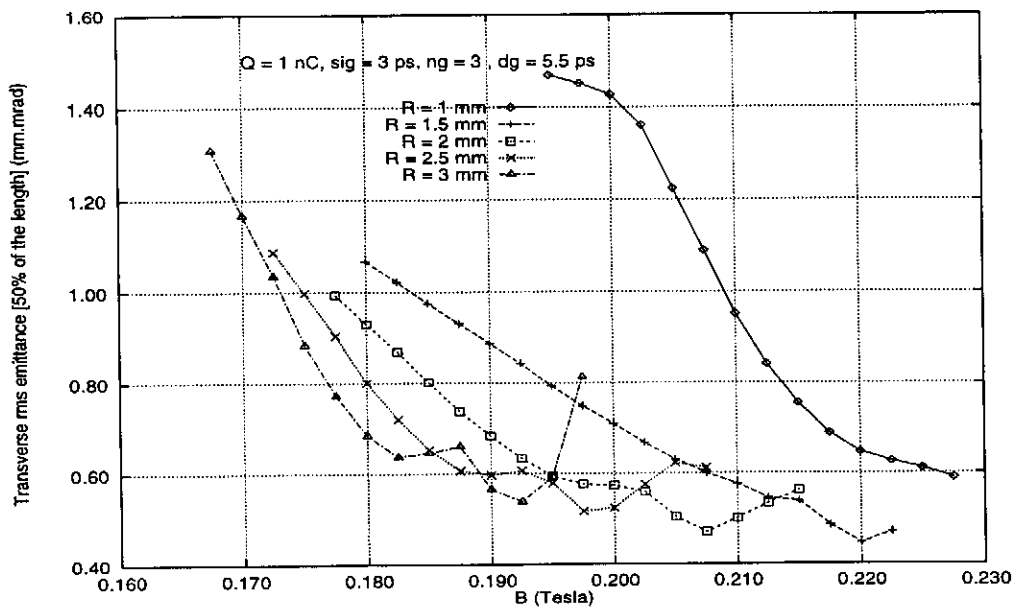


Figure 16: Minimum Transverse rms emittance, 50% of the length, versus the magnetic peak field.

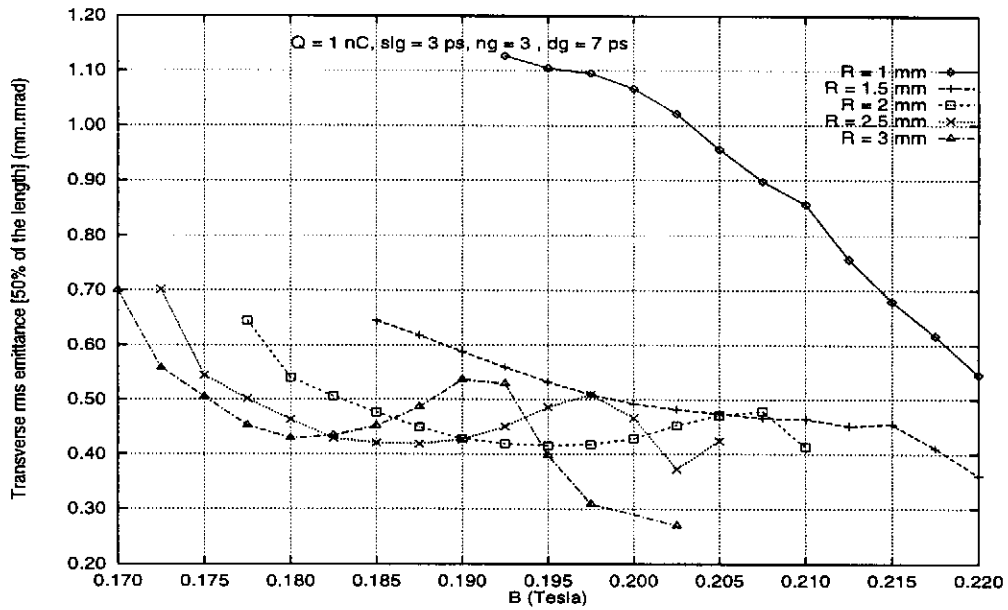


Figure 17: Minimum Transverse rms emittance, 50% of the length, versus the magnetic peak field.

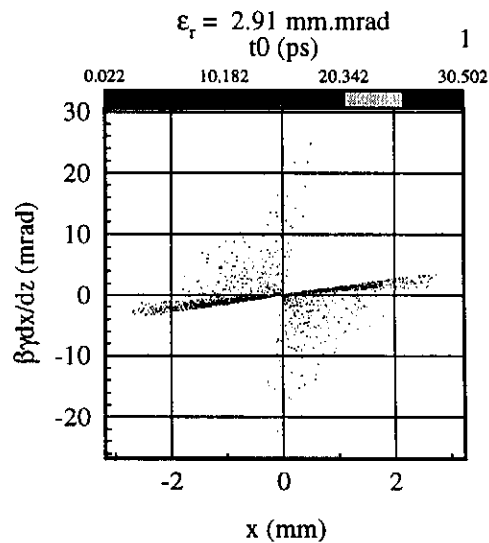


Figure 18: Transverse phase space for the case 3, with R = 2 mm and B = 0.19 Tesla.

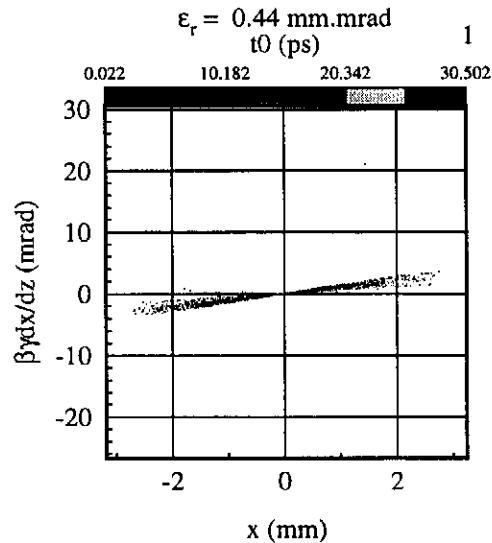


Figure 19: Transverse phase space for the case 3 and 50% of the beam length, with  $R = 2$  mm and  $B = 0.19$  Tesla.

Figures 18, 19 show the transverse phase space for the case 3 with  $R = 2$  mm and  $B = 0.19$  Tesla, for 100% and 50% of the beam length, at  $z = 1.17$  m closed to the minimum  $\epsilon_r^{50\%}$ . We see that the beam tails contribute for 80% of the transverse emittance.

### 3 Longitudinal rms emittance

Figures 20, 21 and 22 show the longitudinal emittance when the radial emittance is minimum, as a function of the magnetic peak field for the cases [1-3]. This different curves have large fluctuations, because :

- all this points are not at the same position, the transverse emittance minimum moves with the magnetic field,
- the longitudinal emittance is greatly dependent on the rms radius evolution.

We can see that the case 1 gives a greater longitudinal emittance than the two other cases. This is due to the discontinuity of the uniform profile, which introduces a non linear effect on the longitudinal phase space, see figure 23. For the case 2, figures 16 and 21 show that we can achieve our objective i.e  $\epsilon_r < 1$  mm.mrad and  $\epsilon_z < 20$  mm.KeV, for  $1.5 < R < 3$ . mm. For the case 3, the second condition is reached only for  $R = 1.5$  and 3 mm, and respectively for a magnetic peak field close to 0.19 and 0.2 Tesla. In this part we will see two values of the longitudinal rms emittance due to the 80% and 50% of the beam length,  $\epsilon_z^{80\%}$  and  $\epsilon_z^{50\%}$ , because ATRAP has been just modified to calculate them.

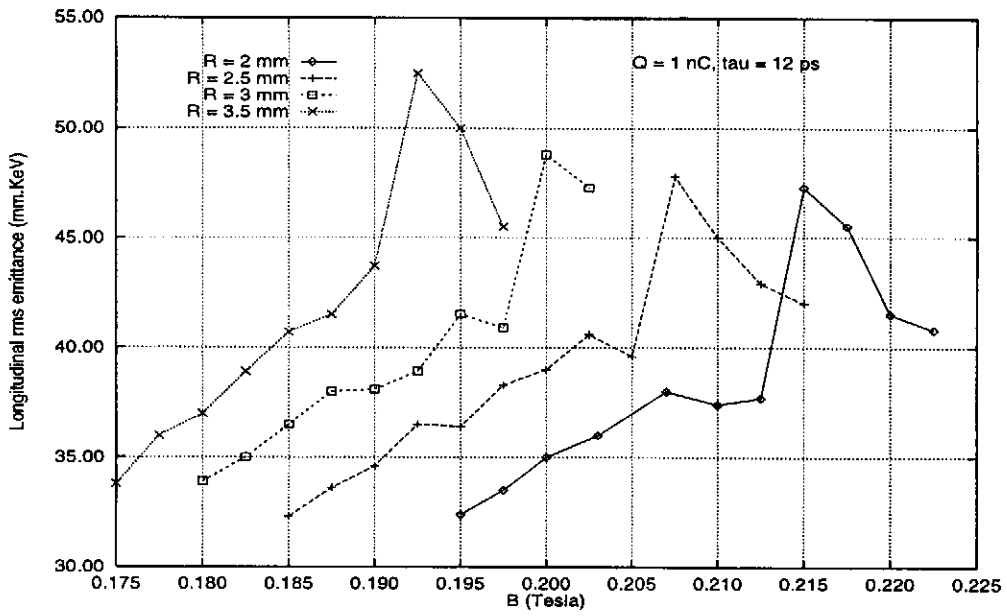


Figure 20: Longitudinal rms emittance when  $\epsilon_r$  is minimum, versus the magnetic peak field.

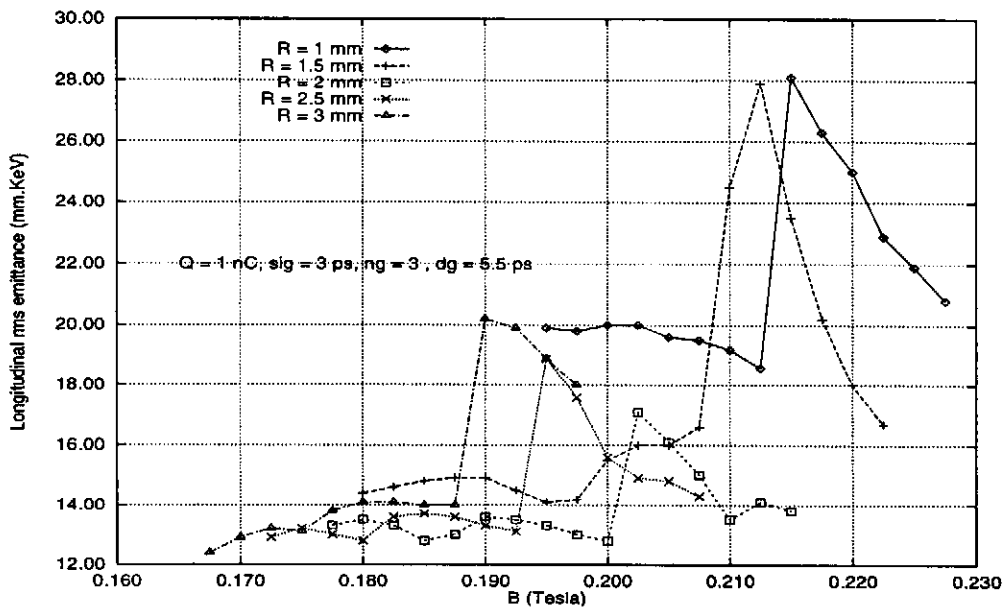


Figure 21: Longitudinal rms emittance when  $\epsilon_r$  is minimum, versus the magnetic peak field.

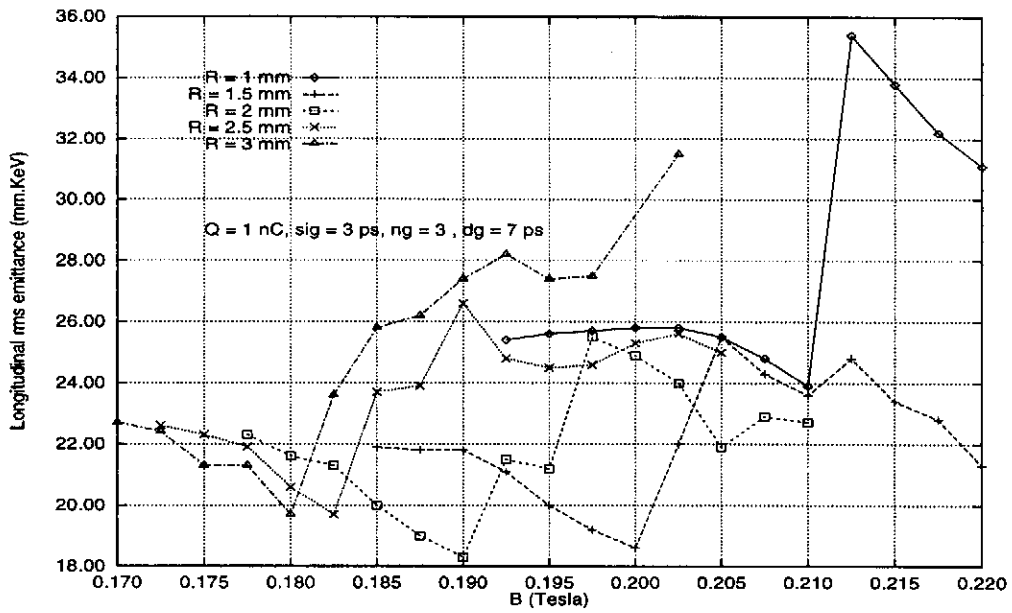


Figure 22: Longitudinal rms emittance when  $\epsilon_r$  is minimum, versus the magnetic peak field.

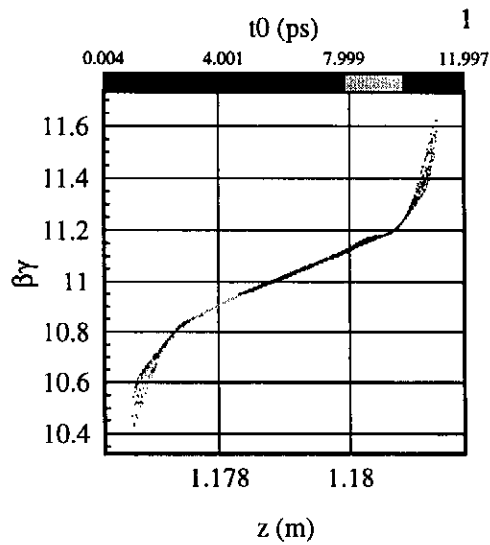


Figure 23: Longitudinal phase space for the cases 1.



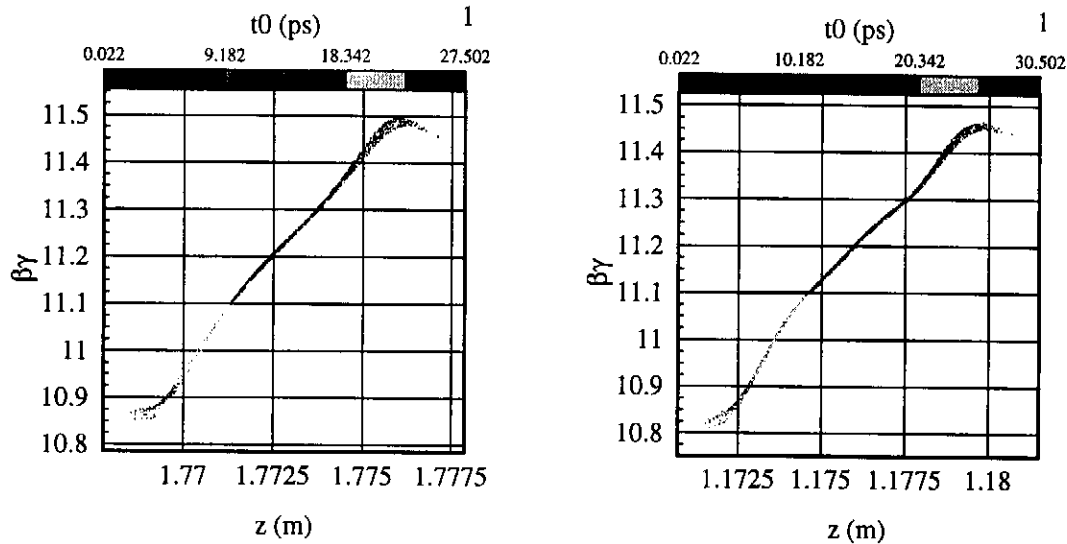


Figure 24: Longitudinal phase space for the cases 2,3.

For the case 2 with  $R = 2$  mm and  $B = 0.185$  Tesla, the simulation gives  $\epsilon_z^{80\%} = 10.7$  mm.KeV,  $\epsilon_z^{50\%} = 4.7$  mm.KeV, and for the case 3, with  $R = 2$  mm and  $B = 0.19$  Tesla,  $\epsilon_z^{80\%} = 16$  mm.KeV,  $\epsilon_z^{50\%} = 4.7$  mm.KeV. There is a factor three between the longitudinal emittances for the total length (see figures 21, 22) and for  $\epsilon_z^{50\%}$ . The longitudinal phase spaces, for the two precedent cases, shown in figure 24, are almost linear except for the edges, and confirm the weak values of  $\epsilon_z^{50\%}$ . Extrapolating these results for the different radii and magnetic peak field, we find that  $\epsilon_z^{50\%}$  is always smaller than 20 mm.KeV.

## 4 Influence of the rf electric field on the cathode

Figure 25 shows the optimized transverse rms emittance versus the magnetic peak field for the case 3 with  $R = 1.5$  mm, and for three different values of the maximum rf electric field  $E_0$  on the cathode. We see that the magnetic field values scales as the rf peak field, because the focussing effect varies like  $B^2/\gamma^2$ , and to keep the same beam evolution, the magnetic peak field must be a growing function of the energy.

The transverse rms emittance for 50% of the beam length is plotted versus the magnetic peak field in figure 26, and goes down when  $E_0$  increases. For  $E_0 = 60$  MV/m on the cathode,  $\epsilon_z^{50\%} = 0.3$  mm.mrad in the flat part of the curve. As we can see in the figure 27, if  $E_0$  is greater than 50 MV/m, the longitudinal rms emittance evolution in function of the magnetic field, is near the same except for the weak values of the magnetic field, where a difference of 10% appears. The case  $E_0 = 40$  MV/m shows that the energy at the gun exit is not sufficient, and when the beam is focused, there is an important effect of the space charge on the longitudinal emittance. These three figures shows that a minimum of 50 MV/m is necessary, if we want to reach our objective.

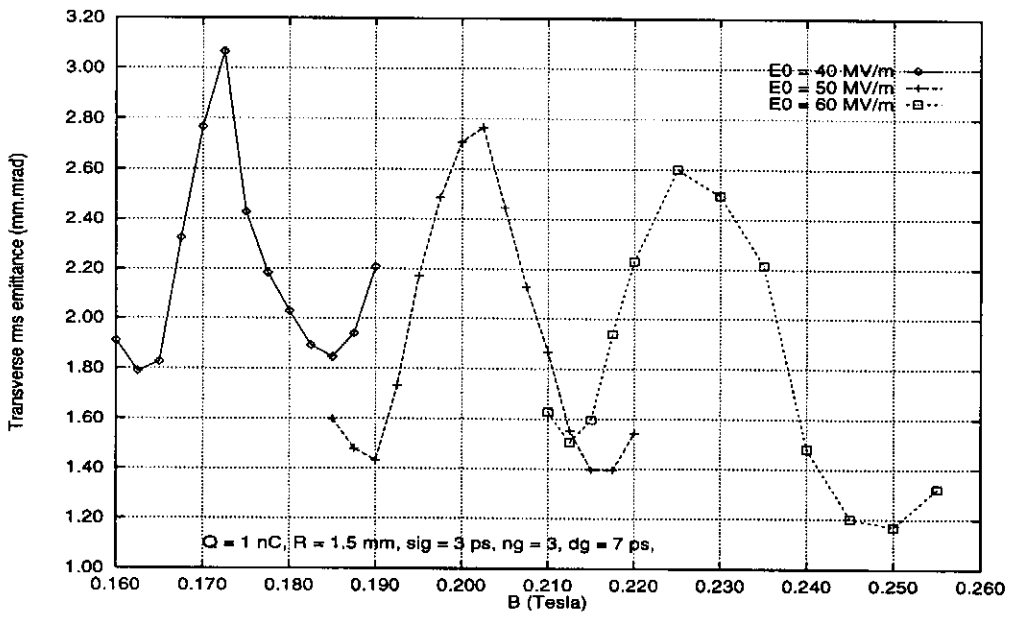


Figure 25: Minimum Transverse rms emittance versus the magnetic peak field.

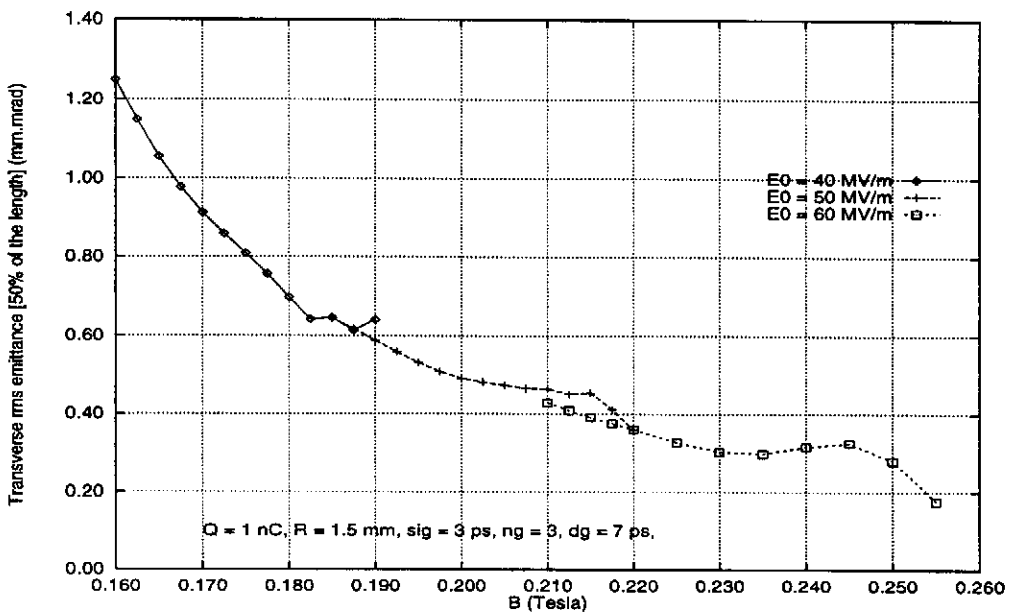


Figure 26: Minimum Transverse rms emittance for 50% of the beam length, versus the magnetic peak field.

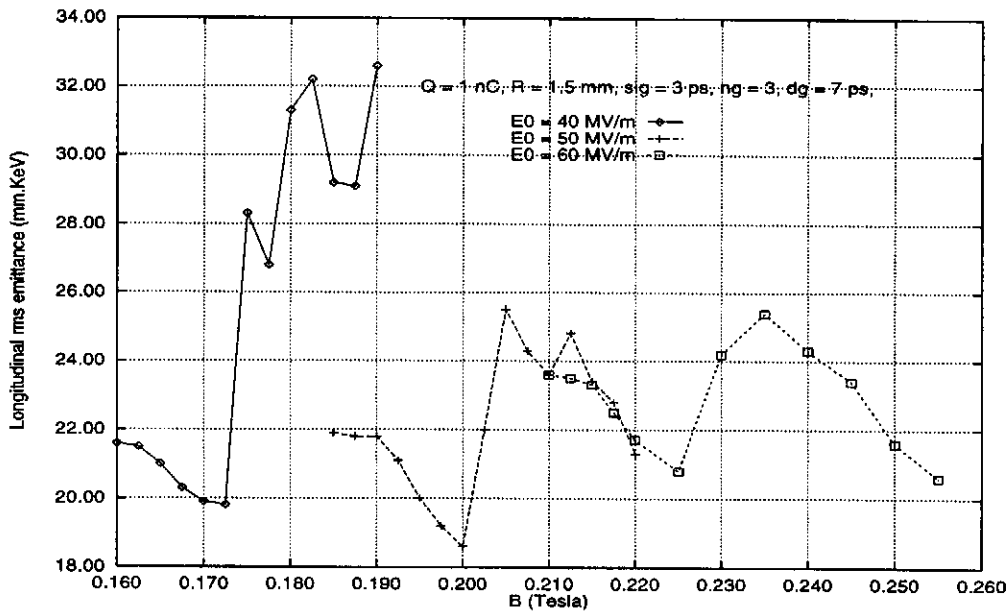


Figure 27: Longitudinal rms emittance when  $\epsilon_r$  is minimum, versus the magnetic peak field.

## 5 Capture Linac influence on the beam quality

Figure 28 shows the rms radius evolution for different values of the solenoid peak field. We have taken the case 3 with  $R = 1.5$  mm, the capture linac is 1.10 m after the photocathode and the maximum peak field is 20 MV/m. The 9 cells position and the rf phase are not well optimized, we have just been careful to have the beam energy closed to the maximum at the capture linac exit, and the minimum of  $\epsilon_r^{50\%}$  after the entrance. The increasing of the curves 3 and 4, after the capture linac is due to the over focusing of the beam edges.

Figure 29 shows the total transverse rms emittance in function of the position, we see clearly an emittance compensation due to the 9 cells cavity. The minimum is 1. mm.mrad for  $B = 0.2025$  and 0.205 Tesla, while this minimum is 1.4 mm.mrad without the capture linac. Furthermore it appears a more stable value in function of the magnetic peak field.

Figure 30 is the transverse rms emittance evolution of 50% of the length. The minimum is 0.5 mm.mrad for  $B = 0.2, 0.2025$  and 0.205 Tesla. In fact the magnetic peak field changes just the position of this minimum.

The longitudinal emittance as a function of the position is plotted in figure 31. After the capture linac  $\epsilon_z$  is between 50 and 60 mm.KeV. It is two or three times the  $\epsilon_z$  value, without capture linac. But if we consider only the 50% of the beam length,  $\epsilon_z^{50\%}$  is closed to 18 mm.KeV.

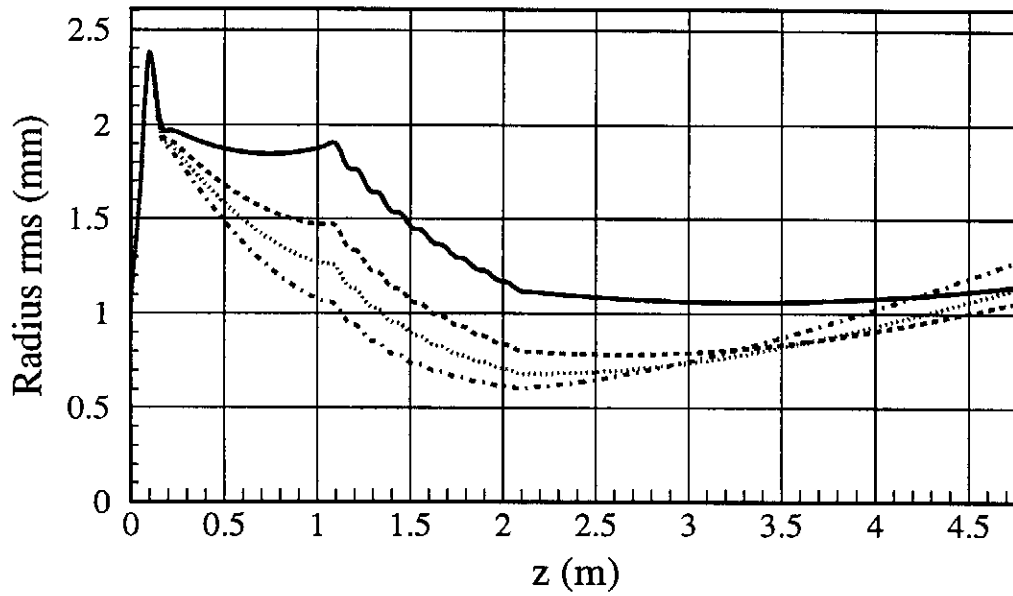


Figure 28: Rms radius in function of the position for different values of the magnetic peak field.

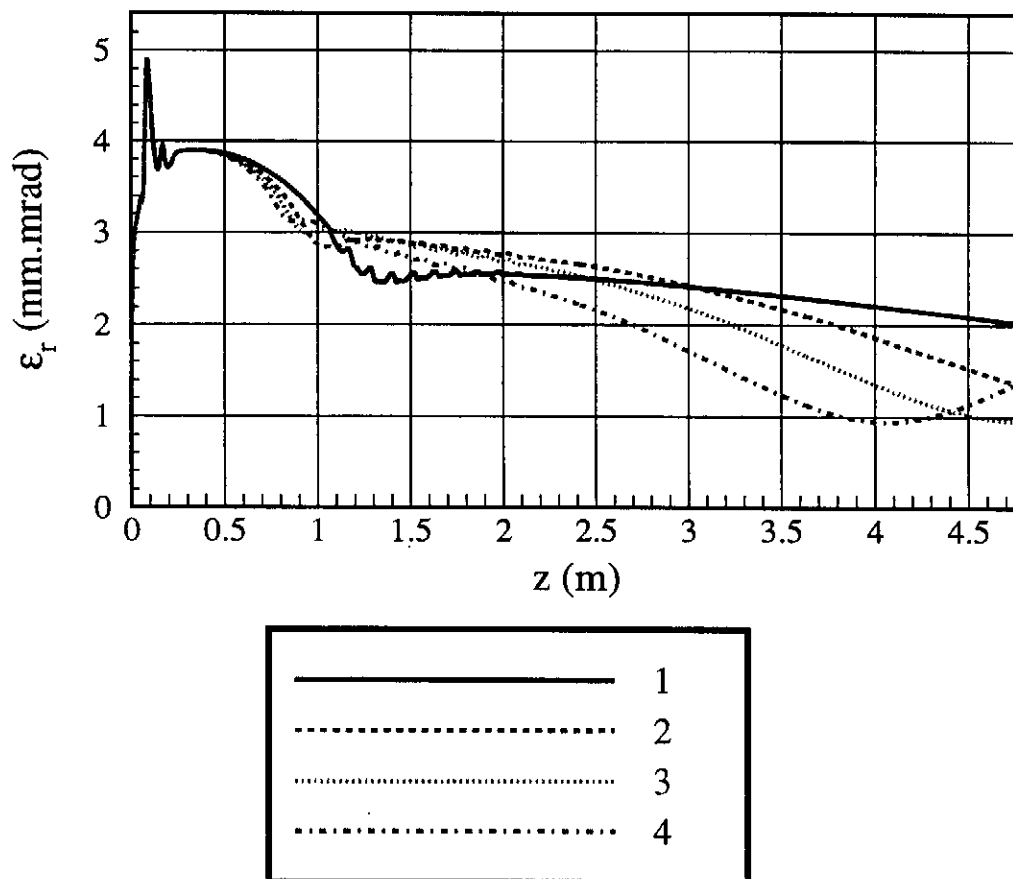


Figure 29: Transverse rms emittance in function of the position for different values of the magnetic peak field : 1, 2, 3, 4 respectively for  $B = 0.195, 0.20, 0.2025, 0.205$  Tesla .

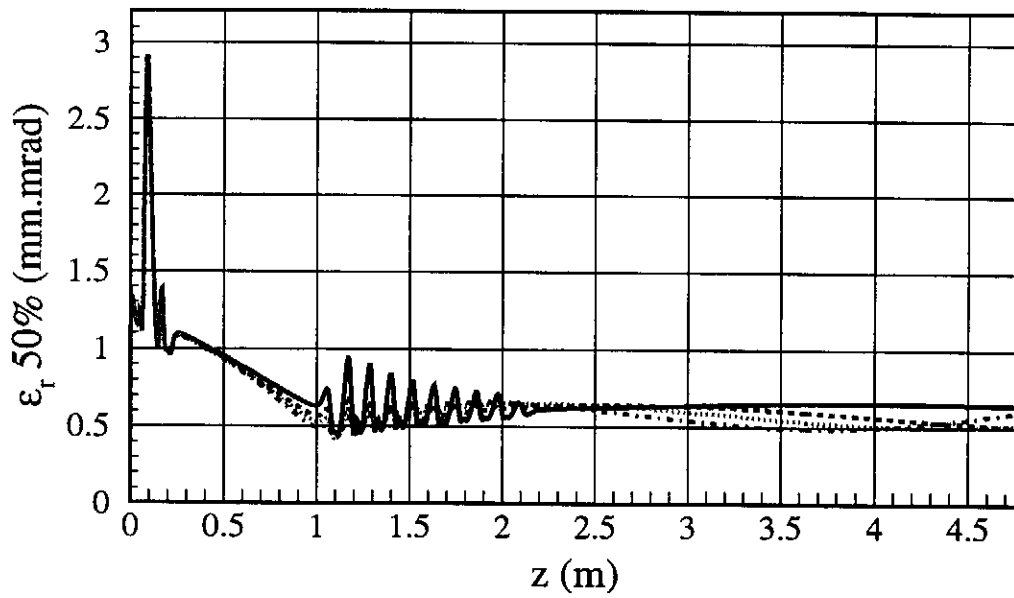


Figure 30: Transverse rms emittance for 50 % of the beam, in function of the position for different values of the magnetic peak field.

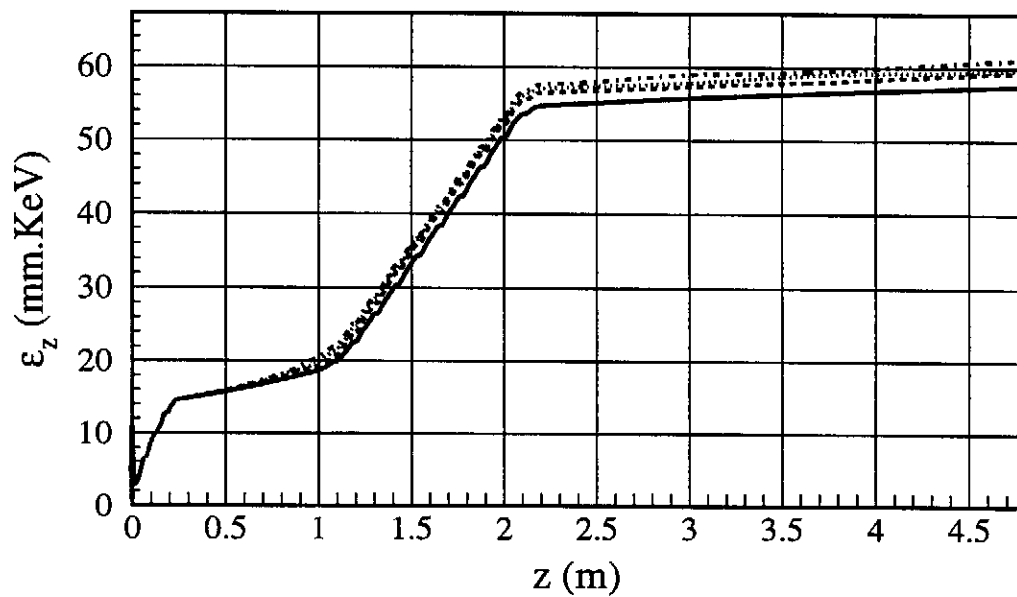


Figure 31: Longitudinal emittance in function of the position for different values of the magnetic peak field.

## 6 Thermal emittance

In the preceding parts, we have not taken into account the thermal emittance, because it is a 3D effect and ATRAP simulates only the 2D1/2 problems. Furthermore the thermal emittance for a semiconductor like the Cs<sub>2</sub>Te photocathode is little known and some measurements must be done. To have an idea of the thermal emittance size, we suppose that the velocity distribution is uniform as the thermionic cathode, and the current density is uniform. To be coherent with the previous definition, we take  $\epsilon_{th} = \frac{1}{2mc} \sqrt{\langle r^2 \rangle \langle pr^2 \rangle}$ ,  $\langle rpr \rangle = 0$  because the phase space (r, pr) is uncorrelated at the photocathode.

With our definition, the thermal emittance is :

$$\epsilon_{th} = \frac{R}{2} \sqrt{\frac{kT}{mc^2}}, \quad (2)$$

with R, the cathode radius and kT the mean energy of the photoelectrons. If we take R = 1.5 mm and kT ≈ 0.9 eV,  $\epsilon_{th} \approx 1$  mm.mrad, which is two times the best transverse emittance for 50% of the beam length, and for the case 3 with the same radius. If the thermal effect and the dynamics effect are uncorrelated, we can define the total emittance by :

$$\epsilon_{tot} = \sqrt{\epsilon_{th}^2 + \epsilon_r^2}, \quad (3)$$

and with our parameters we find  $\epsilon_{tot} = 1.1$  mm.mrad.

## 7 Conclusion

From the simulation results exposed in this paper, the Floetmann's photoinjector seems to be a good candidate to reach our objective :  $\epsilon_r < 1$  mm.mrad and  $\epsilon_z < 20$  mm.KeV at the gun exit. An unconventional temporal distribution like a gaussian superposition with  $\sigma_t = 3$  ps, and a flat top fluctuation close to 5% gives 0.5 mm.mrad for the transverse rms emittance, if we consider only 50% of the beam length.

This compromise between a uniform and gaussian temporal distribution conserves the positive aspect of each : the transverse phase space is less opened for the first, and the longitudinal phase space is more linear for the second. From the point of view of the dynamics, it seems that  $\epsilon_r < 1$  mm.mrad is possible; now the major causes of the beam degradation are technological as the laser stability, or due to the thermal emittance. With a simple model, the thermal emittance is 1. mm.mrad with a 1.5 mm for the beam radius, and two times the dynamics emittance. If we want to optimize this value, we will oblige to decrease the beam radius and consequently to increase the rf peak field on the cathode to minimize the space charge effects.